FMRC Task 2.2b Simulate Eco-Driving Energy Savings

1. Introduction

An eco-approach and departure (EAD) strategy aims to reduce vehicle energy loss and idling time by enabling continuous vehicle motion in urban signalized corridors (Altan et al., 2017; Mintsis et al., 2023). It computes optimal trajectories based on real-time traffic states and traffic signal control plans. A connected automated vehicle (CAV) can obtain mobility and energy benefits when closely tracking the optimal trajectory. Most reported EAD policies rely on a centralized manager to collect traffic flow data, generate reference trajectories, and distribute the trajectories to target vehicles. In addition to benefiting CAVs, these policies use them as actuators to implement the optimal trajectory for their human-driven followers. This can lead to the overall improvement of intersections operation, making EAD a promising active traffic management technology to improve the traffic flow containing both automated and manually-driven vehicles (MDV).

The reported automated vehicle EAD studies usually envision an ideal setting where all vehicles perform car-following movements on one-way intersections, and their real-time states are always available. Many studies require a fully connected automated environment to implement EAD. Those studies neglect real-world operational conditions such as lane change, multi-movement intersection configuration, partially automated fleet, and/or limited traffic state awareness. These conditions represent constraints that must be considered in EAD's real-world deployment. This study aims to develop an EAD algorithm that handles these real-world deployment constraints. The proposed algorithm uses a model predictive controller (MPC) to minimize vehicle speed reduction and variation based on the real-time traffic signal states and queue status measured at the intersection. The required inputs are readily available at modern intersections, and our approach does not require a total CAV environment and ubiquitous traffic monitoring. The proposed controller adopts a generic vehicle state space model that avoids counting vehicle powertrain differences. It makes the controller helpful to both gasoline and electric vehicles, which coexist on the existing road network. Additionally, we implement the controller in a feedback loop to handle traffic state updates due to lane changes and queue propagations. The safety of the EAD algorithm is guaranteed by running an adaptive cruise controller in parallel to the vehicle. The adaptive cruise controller can handle cuttings and preceding vehicles' hard brakes that occasionally happen during an EAD operation.

The field deployment of EAD also requires assistance from traffic management strategies because an EAD controller does not affect MDVs' lane-changing behaviors or resolve the competition between the through and left-turn vehicles. This motivated our development of a lane change management strategy and a signal control implementation strategy to facilitate the EAD implementation. The lane change management strategies provide advisories to human drivers so that they may adjust the lane-changing behavior near EAD vehicles. These strategies can help separate the EAD operation and lane-changing maneuvers spatiotemporally, thus reducing disturbances to the EAD operation. The signal control implementation strategy applies lag left-turn signals to resolve the conflict between the through and left-turn vehicles. It can achieve balanced benefits on different intersection movements, making the proposed controller feasible at multi-movement intersections. To the best of the authors' knowledge, no existing

studies have recognized the dissuasive effects of those real-world challenges on EAD implementation or developed countermeasures to address them. This study has filled this critical research gap.

Eco-Arrival and Departure Control

Methodology Framework

As Figure 1 shows, we implement the proposed EAD in a centralized intersection controller. The intersection controller manages the traffic signal control and trajectory planning (TP) in parallel based on the intersection signal phase and timing (SPaT) plan, current signal state, measured queue lengths in each lane, and CAV states. The intersection controller can directly obtain the signal state and measure the queue length using the roadside equipment. It collects CAV states via vehicle-to-infrastructure communications. The two processes may use different update intervals. Usually, the trajectory planning algorithm needs to be updated more frequently than the signal controller. While the signal control design is independent from the trajectory planning, we ask the intersection controller to provide a fixed phase duration and sequence for the current and the next control cycle. It allows the trajectory planning controller to determine non-stop trajectories based on two consecutive green windows of each intersection movement. We do not consider more than two cycles because the green duration in two cycles is usually enough to serve all vehicles on an intersection link.

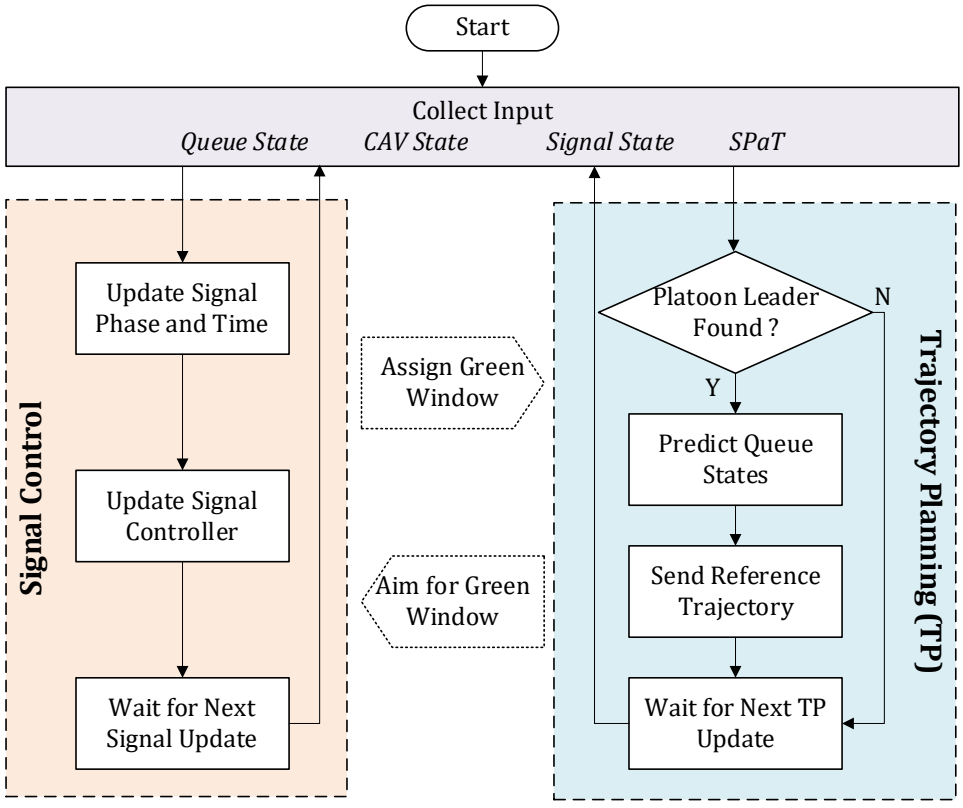

Figure 1. EAD Control Framework.

EAD String Leader Identification

In the TP routine, the intersection controller first identifies the leader CAV of a vehicle string in each lane. A vehicle string is defined as a vehicle group that passes the intersection in the same green window. Our EAD approach relies on individual CAVs as actuators to realize optimal vehicle trajectories for the traffic flow. For this reason, we did not incorporate the states of all vehicles in the problem formulation. Instead, the proposed algorithm only generates optimal trajectories to the leading CAV, letting the cars behind it just follow the leader. This mechanism greatly reduces the computation and communication needs for the proposed algorithm. For this reason, it can reside in the existing connected intersections equipped with standard roadside communication units and roadside processors. Researchers can readily use it in future field tests. We acknowledge that an ideal centralized controller would consider the cost for every vehicle within the intersection region. This is the practice of most existing EAD algorithms. However, this is infeasible when intersections cannot detect MDV states. The all-inclusive consideration also raises computation challenges for real-time operation. Interested readers may refer to (Yao and Li, 2020) for a discussion of all-inclusive optimization.

To identify the string leader CAV, the proposed method defines a passing zone d:

$$d = V \cdot \tau_g \tag{1}$$

where V is the free flow speed; and τ_g is the remaining green time for the considered movement. The passing zone represents a free-driving vehicle's travel distance within the remaining green time. Vehicles inside the passing zone are expected to cross the intersection before the signal turns red. They are not candidates for string leaders. The algorithm selects the first CAV upstream of the passing zone as the string leader to guide the following vehicles to the intersection when the next green window starts. If there is a residual queue at the intersection when the next green starts, the identified string leader will continue tracking the reference trajectory until it crosses the stop bar. In the meantime, the proposed algorithm repeats the string leader search for the next green window. As a result, it forms a new EAD string that is scheduled to pass the intersection in the following green window. We also impose lower and upper distance thresholds in the string leader identification. If a CAV's distance to the intersection does not fall within these thresholds, it cannot be a string leader. The lower distance threshold disqualifies CAVs that cannot execute EAD on a short road segment, whereas the upper bound excludes CAVs that are outside the communication range. If there are no CAVs in the road link, the algorithm will wait until the next CAV arrives.

For each string leader, the proposed algorithm incorporates queue dynamics prediction and optimal trajectory computation in an OCP. We use an MPC framework to solve the OCP in a finite prediction horizon (e.g., 100 s) and repeat the solution process at a small update interval (e.g., 1 s). The length of the prediction horizon should be comparable to the cycle length of a typical signal controller so that the OCP can account for the start times of two consecutive green windows. At an update interval, the controller computes a reference acceleration for the string leader, expecting the vehicle to accelerate during the update interval. This MPC update process happens recursively until the subject vehicle leaves the intersection link. We use the active-set solver offered by Matlab Model Predictive Control Toolbox to search for the solution (Schmid and Biegler, 1994). Additionally, the string leader runs an adaptive cruise controller (ACC) when

tracking the reference trajectory. The ACC ensures car-following safety by overwriting the EAD acceleration if risky conditions occur during an EAD process.

The detailed formulation of the proposed OCP is given in the following subsections.

Vehicle Kinematics

We use the following generic kinematic model to represent the vehicle longitudinal movement. Studies reported by (Bae et al., 2022; Yu and Long, 2022; Zhang et al., 2021) relied on specific models to represent gasoline vehicles, plug-in hybrid vehicles, or electric vehicles, respectively. The traffic flow consists of multiple vehicle classes. A particular vehicle model can bring about tailored improvement for one vehicle type but may not generate positive outcomes for others. The proposed EAD algorithm aims to benefit the overall traffic flow. Therefore, the kinematic model in Equation (2) is applied:

$$\boldsymbol{x}(\boldsymbol{k}+\mathbf{1}) = \begin{bmatrix} s(k+1) \\ v(k+1) \end{bmatrix} = \begin{bmatrix} 1 & \Delta t \\ 0 & 1 \end{bmatrix} \begin{bmatrix} s(k) \\ v(k) \end{bmatrix} + \begin{bmatrix} 0 \\ \Delta t \end{bmatrix} u(k) \tag{2}$$

where k is the time index; Δt is the time step size; s is the vehicle position; v is the speed; u is the desired acceleration; and t represents time. u is the control variable in the proposed OCP.

Control Objective

The proposed OCP uses the objective function in Equation (3) to penalize a string leader's control efforts and speed reduction. The first term on the right-hand side of Equation (3) penalizes the speed variation as a subject vehicle approaches the intersection. The reduction of speed variation can generate energy savings. The second term allows the subject vehicle to travel as close to the free flow speed as possible, thus benefiting mobility. Theoretically, the system reaches the terminal state at infinity. When the OCP is approximated with an MPC approach, we let the terminal time equal the prediction time horizon.

$$Min\ J = \sum_{k=k_0}^{k_f} [\omega_u \cdot u^2(k) + \omega_v \cdot (v(k) - V)^2] \cdot \Delta t \tag{3}$$

where V is defined previously; k_0 is the initial time; k_f is the terminal time; and ω_u and ω_v are weights.

Constraints

Initial state:

At an update interval, the intersection controller collects state of each CAV. This provides the initial condition for a subject CAV:

$$\begin{cases} s(k_0) = s_0 \\ v(k_0) = v_0 \end{cases} \tag{4}$$

where s_0 is the initial position; and v_0 is the initial speed.

Speed and acceleration bounds:

A subject CAV may not drive backward. It also needs to observe the speed limit:

$$0 < v(k) \leq V \tag{5}$$

Note that we require a positive speed for the subject vehicle. This creates continuous vehicle motion. If there is no feasible solution because of this constraint, the subject vehicle will abort EAD and perform normal car-following.

The vehicle has limited acceleration capabilities:

$$a_{min} \leq u(k) \leq a_{max} \tag{6}$$

where a_{min} and a_{max} are the acceleration bounds.

Position constraint:

The red signal and the resulting vehicle queues inflict position constraints on the subject CAV. As Figure 2 shows, the subject vehicle's trajectory should lie under the trajectory of the last queuing vehicle. There are two unique points in the last vehicle's trajectory. Point A is the maximum queue tail: The length of the queue will reduce, and all queued vehicles will start to move after t_A. If the subject vehicle arrives at s_A after t_A, the vehicle can avoid stopping in the queue. Point B marks the condition where the last queuing vehicle passes the stop bar. The subject vehicle should pass the stop bar closely after t_B to ensure the efficiency of queue discharge.

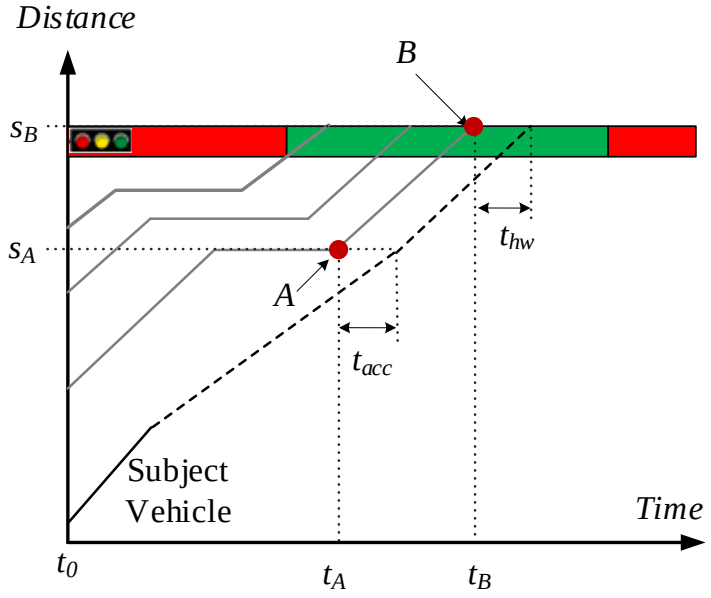

Figure 2. Position constraint for a subject CAV.

With the above discussion, the position constraint is formulated in Equations (7) and (8):

$$0 \le s(k) \le g(k) \tag{7}$$

$$s(k) = s_0 + \sum_{k=k_0}^{k_f} v(k) \cdot \Delta t \tag{8}$$

The upper bound $g(k)$ defined in (9) is a piecewise continuous function representing the combined effects of the signal control and queue:

$$g(k) = \begin{cases} s_A & t_0 \le k \le t_A + t_{acc} \\ s_B & t_A + t_{acc} \le k \le t_B + t_{hw} \\ \infty & k \ge t_B + t_{hw} \end{cases} \tag{9}$$

In Equation (9), t_A, t_B, s_A, and s_B are defined in Figure 2. t_{acc} represents the time when the last queued vehicle accelerates to the speed limit. We assume that the last vehicle keeps an estimated acceleration a_{est} during the process. t_{acc} adds a buffer time so that when the subject vehicle arrives at s_A, all queued vehicles are driving close to the free flow speed. It reduces the likelihood of the subject vehicle braking to ensure car-following safety when joining the queue. Equation (9) also adds t_{hw} to t_B to allow a proper headway between the queue tail and the subject vehicle. If there is no queue, $t_A = t_B = t_g$, $s_A = s_B = s_S$, and $t_{acc} = t_{hw} = 0$, where t_g is the green start, and s_S is the position of the stop bar.

Points A and B are unknown. We use empirical models to estimate those points (i.e., t_A, t_B, s_A, and s_B) based on the signal plan and the queue state measured at t_0. The queue state (i.e., queue length and number vehicles in the queue) is the output from the intersection sensors. We did not limit the type of intersection sensors in our study. The proposed approach is compatible with any intersection detection technologies capable of providing the vehicle number and queue length. This distinguishes the proposed approach from most existing EAD methods that require measurements of all vehicles in the control region. Additionally, our approach does not require detailed queue dynamics models to construct the trajectory of the queue tail, thus reducing the complexity of the OCP formulation. Among the four variables that define A and B, s_B is always the same as s_S. During an update interval Δt, we assume that s_A is a constant equal to the queue length measured at t_0. This simplifies the real-world condition since the queue length may change due to lane changes or new vehicle arrivals. Nonetheless, since our algorithm updates in a short interval (e.g., 1s), the new measurements in the next update interval can promptly capture the queue length change. At oversaturated intersections, the queue could grow beyond the intersection detection range. Such a condition will invalidate the queue tail estimation method. As a result, the proposed EAD algorithm does not work at excessively busy intersections.

We use Equations (10) and (11) to estimate t_A and t_B. The two models may be fitted based on the queue discharge data collected at the intersection. These models formulate t_A and t_B. as functions of the queue length and the number of queued vehicles at t_0. Our analysis of the simulation data shows that these simple regression models can achieve desirable performances (e.g., $R^2 > 0.9$). In real-world applications, one may apply the data-driven approach to update the model parameters online for further performance improvement.

$$t_A = \beta_{A1} + \beta_{A2} \cdot N + \beta_{A3} \cdot L + \beta_{A4} \cdot N^2 + \beta_{A5} \cdot N \cdot L \tag{10}$$

$$t_B = \beta_{B1} + \beta_{B2} \cdot N + \beta_{B3} \cdot L + \beta_{B4} \cdot N^2 + \beta_{B5} \cdot N \cdot L \quad (11)$$

where βs are model coefficients; N is the number of vehicles in queue; and L is the queue length.

Traffic Management Strategies

We hope EAD can create instant benefits for the existing road network. But there is a fundamental barrier. The traffic rules were developed to regulate human driver behaviors, and human drivers form a driving pattern given the constraints of the traffic regulations. Our road system has reached an ecological balance that sustains the interrelationships between the two forces. When EAD creates a new driving behavior, such a balance is disrupted, possibly leading to undesired system performance. In fact, our analyses in the next section reveal negative EAD impacts because the lane change behaviors and signal control practices commonly seen in everyday traffic are at odds with the EAD operation. We, therefore, designed two traffic management strategies to tackle the conflicts, allowing the realization of the expected EAD benefits. The first strategy handles traffic flow downgrades caused by interactions between the EAD driving and lane changes. The second strategy alleviates left-turn traffic's performance reduction due to the EAD operation for the through traffic.

Lane Change (LC) Strategy

The LC strategy provides two sets of advisory messages to human drivers. Transportation agencies may use message signs to display those advisory messages. The first message encourages drivers to stay within an EAD string instead of bypassing it via multiple lane changes. Drivers can easily experience the differences between the two decisions: Staying in the vehicle string leads to a non-stopping intersection cross, whereas making lane changes results in vehicle idling in the queue. MDVs should happily follow the advice once the drivers gain enough exposure to EAD. This strategy only provides recommendations that do not forbid lane changes. Especially when the queue lengths are substantially different on different lanes, drivers should make lane changes to help balance the queue length.

In traffic modeling, the effects of the first advisory message are captured by changing human drivers' discretionary lane-changing thresholds. When the threshold is low, drivers become sensitive to the speed gain in the adjacent lanes. As a result, they tend to make lane changes to bypass the (slow-moving) EAD string instead of staying in the string. On the other hand, a high lane-changing threshold increases the probability for drivers to stay in the EAD string. Additionally, we use a random variable to depict the distribution of the lane-changing threshold in the MDV fleet. The mean level of the random variable will increase when the advisory message is displayed. This modeling method can depict the stochastic lane-changing behaviors with or without the advisory message. The readers may find the details of the traffic modeling in our previous work (Liu et al., 2018).

The second message aims to separate drivers' mandatory lane changes and the EAD operation. Mandatory lane changes happen when a driver needs to move toward the turning lane. As a CAV starts EAD, the following vehicles will form dense vehicle strings. The strings make it difficult for lane change vehicles to identify available gaps in the target lane. Those lane changers must often make last-minute lane changes as the vehicles are discharged from the

intersection. These lane changes will affect the intersection discharging rate, leading to a reduction in the intersection throughput. To address this challenge, the transportation agency may make the EAD control zone shorter than the available intersection link. In this case, the EAD operation does not interfere with the traffic stream in the upstream portion of the intersection link. Additionally, we may display a 'Lane-Change Recommended' message at this segment of the intersection link. Consequently, drivers are encouraged to complete the mandatory lane changes upstream from the EAD zone. This reduces the interaction between the EAD operation and the mandatory lane changes.

We model the effects of the second advisory message by using drivers' anticipatory lane-changing behavior (Liu et al., 2018). The anticipatory lane-change describes drivers' proactive gap searching and lane-changing behavior before they reach the turning lane. When the advisory message is displayed, drivers will start the anticipatory lane-changing behavior at the above lane-changing zone. Since the drivers' anticipatory lane-changing decision is stochastic, we depict the decision-making by using a random variable. As a result, some drivers will make lane changes proactively in the lane-changing zone, while others will change the lane normally.

Left-Turn (LT) Strategy

When there is a need for a protected left-turn signal, most signal controllers implement the lead left-turn signals. This left-turn signal releases the turning traffic before the through traffic, thus reducing conditions where the left-turn queue propagates from the left-turn lane to the through lane and blocks the through flow. However, as we analyzed in Section 1, such a signal control can trap left-turn vehicles in the through EAD strings. Therefore, the LT strategy implements a lag left-turn signal to allow the left-turn vehicles to catch up with the green window after the through vehicles are released. The lag left-turn signal is widely applied in coordinated signal controllers because it allows intersections to accommodate flow progression (Urbanik et al., 2015). We share a similar need as EAD promotes flow progression by using CAVs as actuators. The control technique for coordinated signals is useful for our application.

Evaluation of the Proposed Approach

Study Setup

The studied road network is shown in Figure 3. The network contains two intersections with independent fixed-time signal controllers. Figure 3 also displays the signal phase and timing information. Note that the two intersections are not coordinated. Consequently, most vehicles from the upstream intersection must stop at the downstream intersection due to the lack of green window offset. The eastbound and westbound links serve 1000 vehicles per hour, and the southbound and northbound links serve 250 vehicles per hour. The input flow results in a busy near-saturated intersection operation, and therefore cycle failures occasionally happen at these intersections. We assume the same turn ratios at the two intersections: 75% through, 10% right-turn, and 15% left-turn traffic for the eastbound and westbound, and 15% through, 35% right-turn, and 50% left-turn traffic for the northbound and southbound.

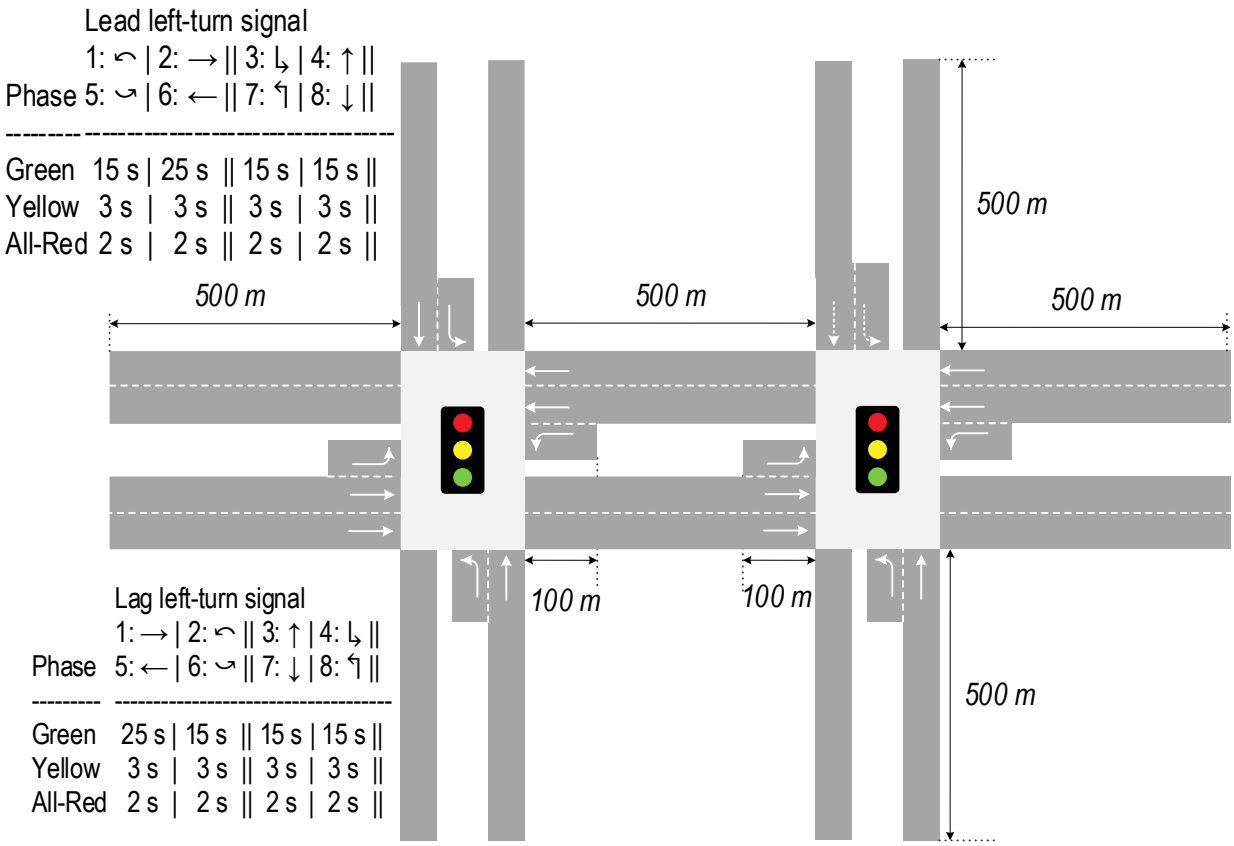

Figure 3. Study Road Network.

The study network and the proposed EAD approach were coded in a simulation environment reported in our previous studies (Liu et al., 2019, 2018). The simulated traffic stream contains both the MDVs and CAVs. The CAVs are assumed to implement the EAD trajectory when selected as the EAD string leaders. Otherwise, they perform ACC car-following or cooperative ACC car-following depending on whether the preceding vehicle is an MDV or CAV. The MDVs implement the PATH car-following and lane change models reported in (Yeo et al., 2008). The proposed traffic management strategies were also programmed into the simulation environment. We considered five analysis cases: 1) a baseline case without EAD; 2) an EAD case without traffic management strategies; 3) an EAD case with the LC strategy; 4) an EAD case with the LT strategy; 5) and an EAD case with both the LC and LT strategies. The varying CAV market penetrations (MPR) were also counted. We evaluated both traffic mobility performance and vehicle energy consumption. The energy consumption was computed by Autonomie (Argonne National Laboratory, 2021). To help readers reproduce the analysis, we list the model parameters in Table 1.

Table 1 Model parameters used in the simulation study.

Parameter	*Value*
V	12 m/s

a_{min}	-3 m/s^2
a_{max}	2 m/s^2
a_{est}	2 m/s^2
t_{hw}	1.5 s
β_{A1} - β_{A5}	-2.14, 1.32, 5.68×10^{-4}, 9.91×10^{-3}, 2.05×10^{-3}
β_{B1} - β_{B5}	1.25, 1.38, 0.12, 9.10×10^{-3}, 1.51×10^{-3}

Effects of EAD without Traffic Management Strategies

First, we investigate the performance of EAD in the existing traffic ecosystem. In this scenario, drivers are inclined to make lane changes if the traffic flows faster in the adjacent lane. The signal controller uses the default lead left-turn signals (see Figure 3). We assume a 40% CAV MPR, which makes EAD effective in most signal cycles. The travel time and the vehicle fuel consumption rate are given in Table 2. The mobility and energy consumption performance drops with EAD. This confirms our previous discussion that implementing EAD in the existing traffic system does not necessarily provide improvement. Our analysis challenges most EAD studies that claim significant EAD benefits whenever it is implemented in the traffic stream. In the following subsection, we show that the proposed traffic management strategies can significantly change this circumstance.

Table 2 Travel time (TT) and fuel consumption rate (F) with and without EAD.

	TT (s/km)	**F (g/km)**
Baseline	145.8	47.4
EAD	161.5	49.1
Δ	+10.8%	+3.5%

Effects of EAD in the Presence of Traffic Management Strategies

Since the LT strategy uses lag left-turn signals, we also adopt lag left-turn signals in the comparison scenarios to make a fair result analysis. The travel time and fuel consumption for different scenarios are shown in Table 3, and the change percentage is listed in Table 4. In addition to the overall performance, we provide matrices for the major through, major left-turn, and minor roads. The detailed information describes the intersection operation comprehensively. The tables reveal a general trend: the LC strategy helps boost the EAD effectiveness, while the LT strategy creates a balanced performance among individual intersection movements.

Table 3 EAD effects in the presence of traffic management strategies.

	TT	**TT_MA**	**TT_ML**	**TT_MI**	**F**	**F_MA**	**F_ML**	**F_MI**
Baseline	145.8	155.9	143.6	165.7	47.4	50.4	50.0	44.0
EAD	161.5	161.9	210.0	199.7	49.1	49.6	61.7	51.2

EAD+LC	164.5	166.1	209.1	201.3	47.7	48.2	59.1	51.3
EAD+LT	154.8	168.3	165.1	160.7	48.5	51.5	55.0	44.5
EAD+LC+LT	153.8	166.9	162.3	160.8	45.9	47.7	50.6	44.6

TT: travel time (s/km); F: fuel consumption rate (g/km); MA: major through; ML: major left;

MI: minor road; LC: lane change strategy; LT: left-turn strategy

Table 4 Performance change percentage in comparison to the baseline case.

	TT	**TT_MA**	**TT_ML**	**TT_MI**	**F**	**F_MA**	**F_ML**	**F_MI**
EAD	10.8%	3.8%	46.3%	20.6%	3.5%	-1.4%	23.5%	16.3%
EAD+LC	12.9%	6.6%	45.6%	21.5%	0.6%	-4.4%	18.4%	16.5%
EAD+LT	2.4%	3.8%	0.2%	0.5%	0.7%	0.5%	4.0%	2.7%
EAD+LC+LT	1.7%	2.9%	-1.4%	0.5%	-4.7%	-6.8%	-4.2%	2.8%

TT: travel time (s/km); F: fuel consumption rate (g/km); MA: major through; ML: major left;

MI: minor road; LC: lane change strategy; LT: left-turn strategy

With the two traffic management strategies, the energy benefits of EAD become prominent. The fuel consumption reduces by 4.7% overall. As expected, the major through movement receives the highest energy savings because it serves the largest traffic volume. A leading CAV can easily extend the energy benefits to the following vehicle strings. The through link also provides a sufficiently long link to allow the EAD strings to execute the reference trajectory. There is little energy saving for the minor road traffic. The minor traffic demand is small, which results in a sparse arrival pattern in the through link. Such an arrival pattern does not favor the EAD string formation. The green window for the minor road is also shorter than the major road. This reduces the solution space of the OCP, increasing the chances that the intersection controller aborts the EAD operation. Those factors explain the lack of energy savings for minor movements.

Without the lag left-turn signal, the travel time of the major left-turn vehicles increases by 46%. It confirms that the left-turn performance significantly decreases due to the EAD operations for the through traffic. When a traffic controller creates very unbalanced effects for different user groups, transport agencies are less likely to accept it for field deployment. The LT strategy greatly improves mobility for left-turn vehicles. The travel time increase drops to 0.2% after the LT strategy is active. The LC strategy can further eliminate the travel time increases. When both strategies are implemented, the travel time reduces by 1.4% for the left-turn movement. One may argue that EAD still negatively impacts intersection mobility. This is expected because the EAD algorithm adds a buffer time in Equation (9) when estimating the queue dynamics. It enables a smooth maneuver as a subject CAV starts to follow the queue tail. But it may increase the headway between the subject CAV and the last queuing vehicle. This increases travel time for the subject CAV and its followers. The travel time increase is hardly

noticeable (e.g., 1.7% on average) and the EAD operation improves drivers' arterial driving experience by facilitating a continuous motion. Our traffic management eliminates the hurdles for implementing EAD on real-world intersection links.

Figure 4 provides a trajectory comparison between the baseline case and the EAD case. Although the CAV MPAR is 40%, most vehicles can avoid stopping at intersections due to the EAD operations. We can also observe frequent lane changes in the baseline case (e.g., partial trajectory curves). Thanks to the LC strategy, the number of lane changes substantially reduces, increasing EAD's capability to create benefits to the traffic stream.

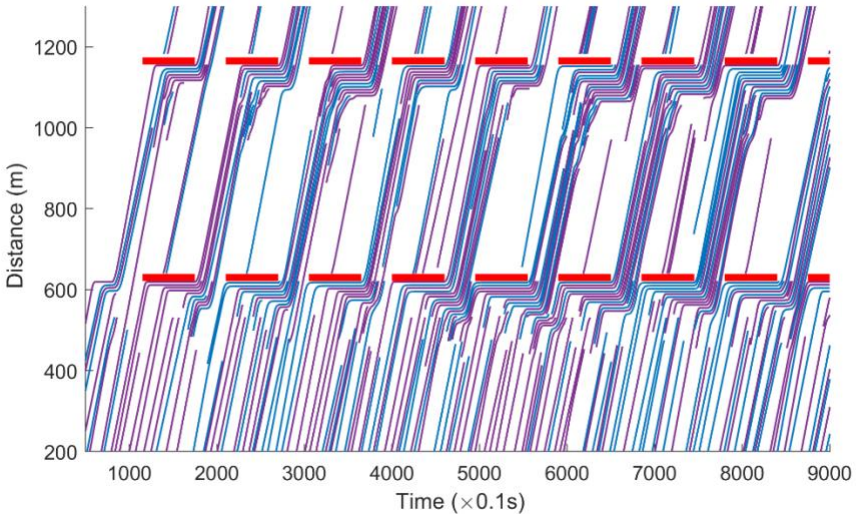

(a)

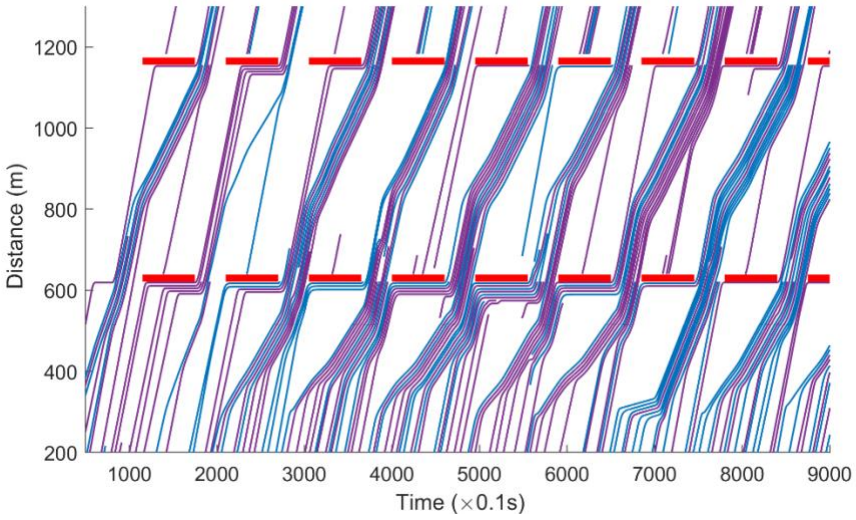

(b)

Figure 4. Vehicle trajectories in the baseline case (a) and EAD+LC+LT case (b). The purple curves depict MDV trajectories, and the blue curves depict CAV trajectories.

Impacts of Drivers' Behavior Adaptation to the Traffic Management Strategies

The proposed LC strategies aim to facilitate EAD operations by modifying human drivers' driving patterns. Their effectiveness depends on how drivers react to the lane-change guidance. We developed a sensitivity analysis to quantify the impacts of driver behavior adaptation on the EAD performances. The driver's behavior adaptation is associated with two random variables: the speed sensitivity and the distance sensitivity. Both sensitivity parameters are assumed to follow a normal distribution with certain mean and standard deviation levels. The speed sensitivity depicts how drivers react to the speed difference between the current and target lanes. If the speed difference is larger than the sensitivity level, the driver will start making a lane change toward the target lane to earn a speed advantage. We formulated such a behavior as:

$$\Delta_v = \frac{V_c - V_t}{V} \geq \theta_v \tag{12}$$

Where Δ_v is the speed difference; V_c is the average speed of the current lane; V_t is the average speed of the target lane; V is the free-flow speed; and θ_v is the speed sensitivity. The distance sensitivity θ_d represents a threshold distance to the intersection. When a driver's distance to the intersection is smaller than the threshold, and his/her current lane does not allow the driver to continue the route, the driver will make anticipatory lane changes toward the desired lane. When the distance sensitivity is large, the driver will proactively make lane changes far from the intersection. This is helpful for the EAD operation.

We assume that the mean level of the speed and distance sensitivity parameters reflects the driver's behavior adaptation with proposed LC strategies. A high adaptation level corresponds to a high speed and distance sensitivity. In this case, the driver is more likely to stay in the EAD string without pursuing temporary speed gain in the adjacent lane. The driver also tends to make anticipatory lane changes far upstream from the EAD zone. Our analysis includes four behavior adaptation scenarios depicted in Table 5. The baseline scenario uses the same sensitivity levels as the non-EAD case. It is compared to three scenarios with low, medium, and high adaptation levels. The rest of the simulation parameters were kept the same as the analysis in the previous section (e.g., 40% CAV and EAD+LC+LT).

Table 5 Sensitivity analysis scenarios.

Behavior Adaptation	Mean θ_v	Std. of θ_v	Mean θ_d (m)	Std. of θ_d (m)
Baseline	0.20	0.01	150	30
Low	0.45	0.01	250	30
Medium	0.70	0.01	350	30
High	0.95	0.01	450	30

The sensitivity analysis results are shown in the following table. The results indicate that the proposed EAD control obtains the best performance in the low adaptation scenario. This suggests that the human drivers only need to change their LC behaviors slightly to promote the EAD

operation. This is a promising result because the EAD operation does not require substantial behavior changes from drivers. When the drivers strictly stay in the EAD string by avoiding discretionary lane changes (e.g., high adaptation scenario), the overall traffic mobility and vehicle energy performance are not desirable. This indicates that discretionary lane changes are necessary to create a balanced traffic stream across multiple travel lanes. We cannot completely remove discretionary lane changes when the EAD is on.

Table 6 Mobility and energy results of different scenarios.

Behavior Adaptation	TT	TT_MA	TT_ML	TT_MI	F	F_MA	F_ML	F_MI
Baseline	149.1	160.1	155.3	168.3	46.6	49.6	51.3	46.0
Low	145.2	153.5	152.4	168.9	44.9	46.4	50.1	46.1
Medium	147.4	157.3	153.1	170.1	44.9	46.6	49.3	46.3
High	150.3	161.7	155.1	170.1	45.1	47.0	49.0	46.4

TT: travel time (s/km); F: fuel consumption rate (g/km); MA: major through; ML: major left; MI: minor road; LC: lane change strategy; LT: left-turn strategy

Table 7 Performance change percentage in comparison to the baseline case.

Behavior Adaptation	TT	TT_MA	TT_ML	TT_MI	F	F_MA	F_ML	F_MI
Low	-2.7%	-4.1%	-1.9%	0.3%	-3.7%	-6.4%	-2.3%	0.1%
Medium	-1.2%	-1.7%	-1.4%	1.0%	-3.7%	-6.1%	-3.8%	0.5%
High	0.8%	1.0%	-0.1%	1.1%	-3.2%	-5.3%	-4.4%	0.8%

Impacts of CAV Market Penetration

We limited our analysis to the 40% CAV case in previous subsections. To understand the effectiveness of the proposed EAD approach, we extended the mobility and energy consumption computation under other CAV MPR cases, especially at low MPR cases. As Figure 5 shows, we investigated more scenarios at the low MPR range than at the high MPR range. It helps us identify the performance of EAD during early-stage deployment. In the EAD case, the LC and LT strategies are turned on.

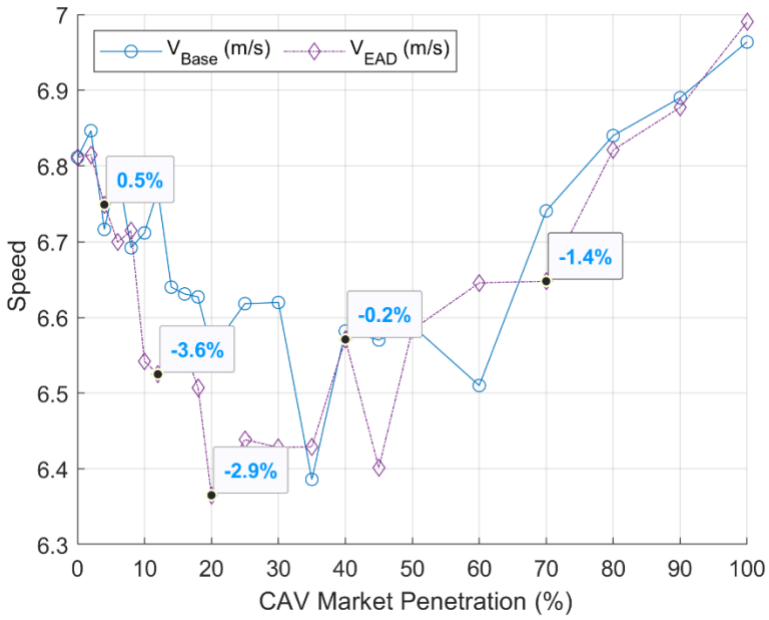

(a)

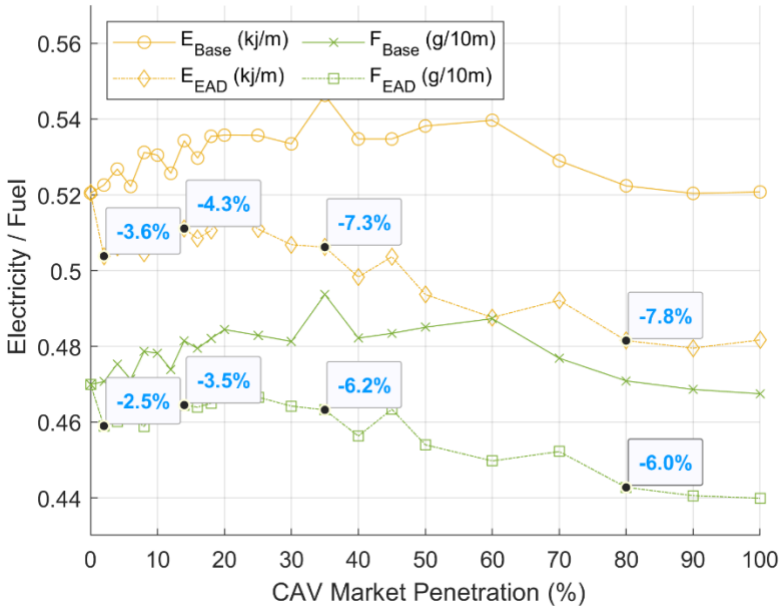

(b)

Figure 5. Average speed (a) and energy consumption (b) at different CAV MPR cases.

Figure 5 indicates that EAD slightly reduces the average speed at low MPR cases. As the MPR is larger than 30%, the negative speed impact diminishes. The largest speed reduction is observed over the 10% to 25% MPR range, and the speed reduction is lower than 4%. On the other hand, the fuel saving ranges from 2.5% to 6.2%. Observing noticeable fuel savings (e.g., 2.5%) in the

2% CAV case is encouraging. Since the EAD operation only requires one CAV leader at each lane to implement the optimal trajectory, it can produce benefits once there are a few CAVs in the traffic stream. The observations suggest that the proposed EAD approach is a promising use case for promoting the early-stage deployment of connected automated vehicle technologies.

Performance of Electric Vehicles and Gasoline Vehicles

Since the proposed EAD algorithm uses a generic vehicle dynamics model, it can provide trajectory guidance for vehicles with different powertrains. Hence, we separately evaluated the energy savings for gasoline and electric vehicles. Figure 5 (b) indicates that electric vehicles obtain higher energy savings than gasoline vehicles under the same CAV MPR. This is certainly good news, given the rapid trend of vehicle electrification. However, it is counter-intuitive because electric vehicles can recycle energy via regenerative braking. When a vehicle comes to a full stop, the electric powertrain loses less energy than the gasoline powertrain. In this case, the energy saving potential should be higher for gasoline vehicles than electric vehicles under the EAD operation. To further examine this observation, one needs to explore the detailed vehicle-level mechanisms for the two classes of vehicles. It is beyond the traffic analysis presented in this study. We leave this matter to future research.

Conclusion

In this study, we have developed a centralized EAD algorithm that enables continuous traffic flow in an arterial network while considering real-world traffic operation constraints, including the partial CAV environment, limited traffic monitoring data, and intersection queue dynamics. We also designed traffic management strategies to allow EAD implementation under challenging conditions caused by vehicle lane changes and different traffic movements' competitions. Compared to the non-EAD case, the EAD approach produces 2.5% to 7.8% energy savings while keeping similar intersection mobility. Notably, our approach brings about 2.5% to 3.6% energy savings in a 2% CAV case. This result demonstrates the feasibility of deploying EAD at low CAV MPR cases.

Implementing EAD in the existing traffic flow may not create benefits because, on the one hand, the prevailing human driving patterns can break the EAD operation, and on the other hand, the EAD operation can intensify the competition between the through and left-turn traffic for the green window. Such an observation reveals the necessity for adapting the existing transportation system to accommodate new CAV technologies. It also shows the importance of performing modeling and simulation studies to help stakeholders proactively identify feasible system adaptation plans. Particularly in this study, we developed lane change and lag left-turn strategies to address the EAD implementation challenges. These strategies only require minor road signage and signal control configuration modifications. The drivers are expected to comply because these strategies can increase driving comfort by reducing lane changes and stop-and-go experiences. Through the study, we prove that transportation agencies can better exploit the capability of CAV applications via cost-effective traffic management policies. Such findings provide a valuable reference for stakeholders to design future CAV development and implementation plans.

References

Altan, O.D., Wu, G., Barth, M.J., Boriboonsomsin, K., Stark, J.A., 2017. GlidePath: Eco-Friendly Automated Approach and Departure at Signalized Intersections. IEEE Transactions on Intelligent Vehicles 2, 266–277. https://doi.org/10.1109/TIV.2017.2767289

Argonne National Laboratory, 2021. Autonomie [WWW Document]. Vehicle & Mobility Systems Department - Argonne National Laboratory. URL https://vms.taps.anl.gov/tools/autonomie/ (accessed 3.21.23).

Bae, S., Kim, Y., Choi, Y., Guanetti, J., Gill, P., Borrelli, F., Moura, S.J., 2022. Ecological Adaptive Cruise Control of Plug-In Hybrid Electric Vehicle With Connected Infrastructure and On-Road Experiments. Journal of Dynamic Systems, Measurement, and Control 144. https://doi.org/10.1115/1.4053187

Feng, Y., He, D., Guan, Y., 2019. Composite Platoon Trajectory Planning Strategy for Intersection Throughput Maximization. IEEE Transactions on Vehicular Technology 68, 6305–6319. https://doi.org/10.1109/TVT.2019.2914163

Feng, Y., Yu, C., Liu, H.X., 2018. Spatiotemporal intersection control in a connected and automated vehicle environment. Transportation Research Part C: Emerging Technologies 89, 364–383. https://doi.org/10.1016/j.trc.2018.02.001

Guo, Q., Angah, O., Liu, Z., Ban, X. (Jeff), 2021. Hybrid deep reinforcement learning based eco-driving for low-level connected and automated vehicles along signalized corridors. Transportation Research Part C: Emerging Technologies 124, 102980. https://doi.org/10.1016/j.trc.2021.102980

Guo, Y., Ma, J., Xiong, C., Li, X., Zhou, F., Hao, W., 2019. Joint optimization of vehicle trajectories and intersection controllers with connected automated vehicles: Combined dynamic programming and shooting heuristic approach. Transportation Research Part C: Emerging Technologies 98, 54–72. https://doi.org/10.1016/j.trc.2018.11.010

Laharotte, P.-A., Bhattacharyya, K., Perun, J., El Faouzi, N.-E., 2023. Traffic-sensitive speed advisory system based on Lagrangian traffic indicators. Journal of Intelligent Transportation Systems 0, 1–23. https://doi.org/10.1080/15472450.2023.2236549

Li, M., Wu, X., He, X., Yu, G., Wang, Y., 2018. An eco-driving system for electric vehicles with signal control under V2X environment. Transportation Research Part C: Emerging Technologies 93, 335–350. https://doi.org/10.1016/j.trc.2018.06.002

Liu, H., Kan, X. (David), Shladover, S.E., Lu, X.-Y., Ferlis, R.E., 2018. Modeling impacts of Cooperative Adaptive Cruise Control on mixed traffic flow in multi-lane freeway facilities. Transportation Research Part C: Emerging Technologies 95, 261–279. https://doi.org/10.1016/j.trc.2018.07.027

Liu, H., Lu, X.-Y., Shladover, S.E., 2019. Traffic signal control by leveraging Cooperative Adaptive Cruise Control (CACC) vehicle platooning capabilities. Transportation Research Part C: Emerging Technologies 104, 390–407. https://doi.org/10.1016/j.trc.2019.05.027

Ma, C., Yu, C., Yang, X., 2021. Trajectory planning for connected and automated vehicles at isolated signalized intersections under mixed traffic environment. Transportation Research Part C: Emerging Technologies 130, 103309. https://doi.org/10.1016/j.trc.2021.103309

Mintsis, E., Vlahogianni, E.I., Mitsakis, E., Aifadopoulou, G., 2023. Advisory versus automated dynamic eco-driving at signalized intersections: lessons learnt from empirical evidence and simulation experiments. Journal of Intelligent Transportation Systems 0, 1–20. https://doi.org/10.1080/15472450.2023.2289118

Schmid, C., Biegler, L.T., 1994. Quadratic programming methods for reduced hessian SQP. Computers & Chemical Engineering, An International Journal of Computer Applications in Chemical Engineering 18, 817–832. https://doi.org/10.1016/0098-1354(94)E0001-4

Soleimaniamiri, S., Ghiasi, A., Li, X., Huang, Z., 2020. An analytical optimization approach to the joint trajectory and signal optimization problem for connected automated vehicles. Transportation Research Part C: Emerging Technologies 120, 102759. https://doi.org/10.1016/j.trc.2020.102759

Sun, C., Guanetti, J., Borrelli, F., Moura, S.J., 2020. Optimal Eco-Driving Control of Connected and Autonomous Vehicles Through Signalized Intersections. IEEE Internet of Things Journal 7, 3759–3773. https://doi.org/10.1109/JIOT.2020.2968120

Urbanik, T., Tanaka, A., Lozner, B., Lindstrom, E., Lee, K., Quayle, S., Beaird, S., Tsoi, S., Ryus, P., Gettman, D., Sunkari, S., Balke, K., Bullock, D., National Cooperative Highway Research Program, Transportation Research Board, National Academies of Sciences, Engineering, and Medicine, 2015. Signal Timing Manual - Second Edition. Transportation Research Board, Washington, D.C. https://doi.org/10.17226/22097

Wang, P., Jiang, Y., Xiao, L., Zhao, Y., Li, Y., 2020. A joint control model for connected vehicle platoon and arterial signal coordination. Journal of Intelligent Transportation Systems 24, 81–92. https://doi.org/10.1080/15472450.2019.1579093

Wang, Z., Wu, G., Hao, P., Barth, M.J., 2018. Cluster-Wise Cooperative Eco-Approach and Departure Application for Connected and Automated Vehicles Along Signalized Arterials. IEEE Transactions on Intelligent Vehicles 3, 404–413. https://doi.org/10.1109/TIV.2018.2873912

Xiao, X., Zhang, Y., Wang, X.B., Yang, S., Chen, T., 2021. Hierarchical Longitudinal Control for Connected and Automated Vehicles in Mixed Traffic on a Signalized Arterial. Sustainability 13, 8852. https://doi.org/10.3390/su13168852

Xu, B., Ban, X.J., Bian, Y., Li, W., Wang, J., Li, S.E., Li, K., 2019. Cooperative Method of Traffic Signal Optimization and Speed Control of Connected Vehicles at Isolated Intersections. IEEE Transactions on Intelligent Transportation Systems 20, 1390–1403. https://doi.org/10.1109/TITS.2018.2849029

Yang, H., Almutairi, F., Rakha, H., 2021. Eco-Driving at Signalized Intersections: A Multiple Signal Optimization Approach. IEEE Transactions on Intelligent Transportation Systems 22, 2943–2955. https://doi.org/10.1109/TITS.2020.2978184

Yao, H., Li, X., 2020. Decentralized control of connected automated vehicle trajectories in mixed traffic at an isolated signalized intersection. Transportation Research Part C: Emerging Technologies 121, 102846. https://doi.org/10.1016/j.trc.2020.102846

Yao, Z., Zhao, B., Yuan, T., Jiang, H., Jiang, Y., 2020. Reducing gasoline consumption in mixed connected automated vehicles environment: A joint optimization framework for traffic signals and vehicle trajectory. Journal of Cleaner Production 265, 121836. https://doi.org/10.1016/j.jclepro.2020.121836

Yeo, H., Skabardonis, A., Halkias, J., Colyar, J., Alexiadis, V., 2008. Oversaturated Freeway Flow Algorithm for Use in Next Generation Simulation. Transportation Research Record 2088, 68–79. https://doi.org/10.3141/2088-08

Yu, C., Feng, Y., Liu, H.X., Ma, W., Yang, X., 2018. Integrated optimization of traffic signals and vehicle trajectories at isolated urban intersections. Transportation Research Part B: Methodological 112, 89–112. https://doi.org/10.1016/j.trb.2018.04.007

Yu, M., Long, J., 2022. An Eco-Driving Strategy for Partially Connected Automated Vehicles at a Signalized Intersection. IEEE Transactions on Intelligent Transportation Systems 1–14. https://doi.org/10.1109/TITS.2022.3145453

Zhang, J., Tang, T.-Q., Yan, Y., Qu, X., 2021. Eco-driving control for connected and automated electric vehicles at signalized intersections with wireless charging. Applied Energy 282, 116215. https://doi.org/10.1016/j.apenergy.2020.116215

Zhou, M., Yu, Y., Qu, X., 2020. Development of an Efficient Driving Strategy for Connected and Automated Vehicles at Signalized Intersections: A Reinforcement Learning Approach. IEEE Transactions on Intelligent Transportation Systems 21, 433–443. https://doi.org/10.1109/TITS.2019.2942014